1 × 12 Unequally spaced waveguide array for actively tuned optical phased array on a silicon nanomembrane

David Kwong,[a] Amir Hosseini, Yang Zhang, and Ray T. Chen[b]
Microelectronic Research Center, Department of Electrical and Computer Engineering, University of Texas, 10100 Burnet Rd. Austin, Texas 78758, USA

(Received 31 March 2011; accepted 12 July 2011; published online 2 August 2011)

We present an experimental demonstration of an optical phased array implementation on silicon nanomembrane. The integrated on-chip array configuration is non-uniform and avoids grating lobes inside the field of view during beam steering while allowing the waveguide separation to be large enough to prevent optical coupling. A 1 × 12 multimode interference beam splitter uniformly excites the arrayed waveguides. Individually controllable micro-heaters modulate the optical phase in the arrayed waveguides. A beam steering angle of 10.2° in a silicon planar guide equivalent to an effective steering angle of 31.9° in air is demonstrated at 1.55 μm. © *2011 American Institute of Physics*. [doi:10.1063/1.3619847]

Traditionally, optical beam steering has been achieved through mechanically controlled MEMS system[1] and liquid crystal (LC) based optical phased arrays (OPAs).[2–4] While mechanical beam steering provides high steering efficiency and relatively large scanning angles, high precision rotating stages are required, which increase the device complexity and are not fast enough for high speed applications. LC OPAs are capable of beam steering without expensive and complex mechanical systems but suffer from low steering speed (~10 ms) and limited steering angle (<10°).[4] Also, increased steering angle causes degradation of the side-lobe level (SLL) and prohibitively coarse angular resolution.[5] OPAs can also be implemented using waveguide arrays. A 2-element waveguide array on GaAs with GHz steering speed was demonstrated with a maximum steering angle of ~6°.[6] A thermo-optically controlled waveguide array fabricated on silicon-on-insulator (SOI) demonstrated a steering angle of 2.3° at a wavelength of 1550 nm.[7]

For uniform OPAs capable of large angle beam steering, an inter-element spacing of about one-half the operating wavelength is required which would result in strong coupling between adjacent waveguides in the array. In order to overcome this trade-off between the maximum steering angle and waveguide spacing for linear uniform arrays, we proposed a non-uniform array consisting of uniform sub-arrays with non-overlapping grating lobes.[5] Also, compared to a uniform array with half-wavelength spacing, the larger total aperture of such an array results in narrower beam width in the far field, which is advantageous for scanning applications.[5] In this letter, we report the implementation of a non-uniform optical array for large angle beam steering.

A schematic of the OPA device on SOI is shown in Figure 1(a), showing both photonic and electronic layers vertically separated by a layer of silicon dioxide for optical isolation. The beam propagation simulation of the photonic circuitry of Figure 1(a) at $\lambda = 1.55$ μm is shown in Figure 1(b). The optical input power is uniformly divided into 12 waveguides using a 1 × 12 multimode interference (MMI) beam splitter, which has a width and length of 60 μm and 553.4 μm, respectively. The input and output access waveguides' widths are 2.6 μm, which has been optimized for high MMI performance.[8] The MMI output access waveguides' widths are adiabatically tapered down to 500 nm over 250 μm length using a linear taper for single mode operation. Previously, we reported that this MMI coupler has an insertion loss of 1.13 dB and uniformity fluctuation within 0.72 dB.[9] The input light is transverse-electrically (TE) polarized that provides higher optical mode confinement compared to the transverse-magnetic (TM) polarization for 500 nm × 230 nm single mode silicon waveguides [Fig. 2(a)]. Also, due to the large index discontinuity at the top and bottom waveguide faces, the TM mode profile has larger vertical spread that reaches the micro-heaters and results in high propagation loss with a 1 μm top cladding of SiO_2.

There are 12 independently addressed 800 nm wide and 500 μm long thermo-optic (TO) phase modulators, as depicted in Fig. 1(a), to provide continuous phase tuning needed for beam steering. Independent phase shifters enable us to reset with modulo 2π phase shifts ($2m\pi + \Delta\theta_n = \Delta\theta_n$, where m is a positive integer and $\Delta\theta_n$ is the phase shift of the nth element).[10] The following passive s-bend phase shifters [Figure 1(b)] compensate for the quadratic MMI beam splitter output phase profile[11] and change the separation of the uniform MMI outputs to that of the non-uniform array. This phase compensation allows the output beam to be steered at 0° when no heat is applied to the 12 phase shifters. The waveguides are then arranged in a non-uniform 12-element array, consisting of 3 four-element uniform sub-arrays, as shown in Figure 2(a). The spacing of each *ith* sub-array s_i is chosen such that there is no overlap of its far-field grating lobes with those of the other sub-arrays.[5] The smallest inter-element spacing is 3.1 μm and the total array size is $A = 46.5$ μm.

The OPA output waveguides are terminated at a 1 cm long silicon planar guide, in which the interference of the light from the 12-channel array results in beam steering at the far field zone. The steering angle is observed along the

[a]Electronic mail: david.kwong@utexas.edu.
[b]Electronic mail: raychen@uts.cc.utexas.edu.

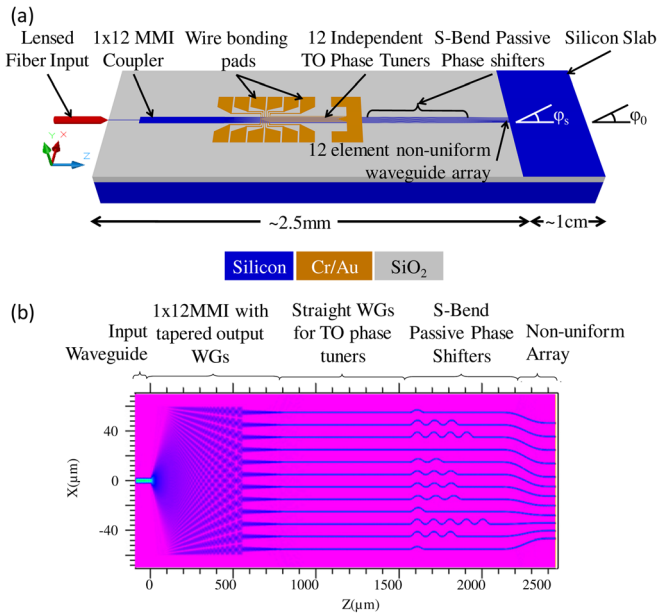

FIG. 1. (Color online) (a) A schematic of the silicon waveguide based optical phased array. (b) Beam propagation simulation of the photonic circuit.

exit side of the planar guide at the chip edge [Figure 1(a)]. For the far field condition to be satisfied, $n_{eff}A^2/(D\lambda) < 1$ is required,[12] where A is the aperture size of the OPA, λ is the operating wavelength, D is the distance of the observation point from the array (here the length of the silicon planar guide), and n_{eff} is the effective refractive index of propagation inside the silicon slab. Similar to the uniform array, the non-uniform array is linearly phased, that is for any nth array element, $\gamma_n/|\bar{d}_n| = r$, where γ_n is the phase applied to the nth element, $\bar{d}_n$ is the position vector of the nth element, and r is a constant. The steering angle inside the silicon planar guide is given as $\varphi_s = \arcsin(\omega\sqrt{\mu\varepsilon_{eff}}/r)$. Note that as the beam reaches the end of the slab and enters free space, its direction is governed by Snell's Law. The theoretical far field patterns for steered and non-steered beams are shown in Figure 2(b).

We used SOI from SOITEC with 3 μm buried oxide (BOX) and 250 nm top silicon layer, which is thermally oxidized to create an oxide etch mask, leaving a final silicon thickness of 230 nm. Electron beam lithography and reactive

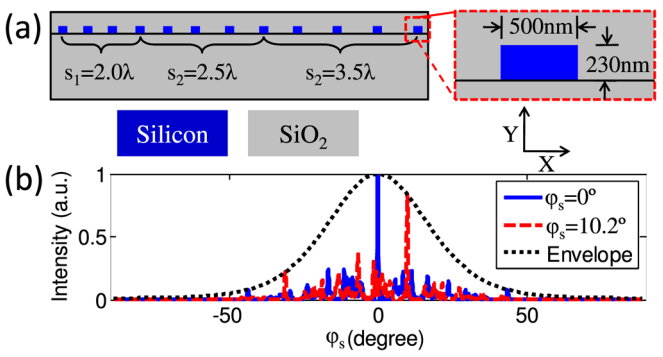

FIG. 2. (Color online) (a) 12-element non-uniform array design with 3 sub-arrays of single-mode silicon waveguides embedded in silicon dioxide, with dimensions of a single waveguide shown in the inset. (b) Theoretical far-field pattern for a non-steered and a steered beam inside the planar guide. The envelope is the far field pattern of a single silicon waveguide embedded in silicon dioxide.

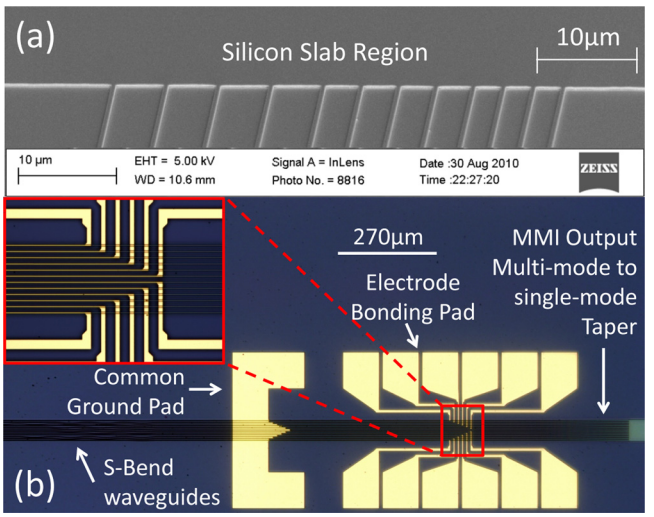

FIG. 3. (Color online) (a) Tilted SEM view of the unequally spaced OPA output and silicon nanomembrane planar guide. (b) Optical microscope picture of the 12 thermo-optic heaters with bonding pads.

ion etching is used to pattern this layer to form the photonic circuitry. A scanning electron microscope (SEM) picture of the interface between the unequally spaced OPA and silicon nanomembrane planar guide is shown in Figure 3(a). Using the Plasmatherm 790, a 1 μm thick film of plasma-enhanced chemical vapor deposition (PECVD) silicon dioxide (325 °C, 80 W, 400 mTorr, 42 sccm N_2O, and 21 sccm SiH_4) was deposited as top cladding, which is sufficient to isolate the TE guided modes from the electrodes to prevent high optical loss. Metal heaters are patterned over the waveguides by e-beam lithography and thermal evaporation and liftoff of 150 nm of Cr/Au [10/140] film. An optical microscope picture of the heaters aligned over the output waveguides and 12 bonding pads is shown in Figure 3(b).

We engineered the "bread loafing" effect in which self-aligned voids are formed during PECVD oxide deposition and are shown in Figure 4(a). COMSOL MULTIPHYSICS simulations in Figure 4(b) indicate the effectiveness of these voids in directing the generated heat toward the silicon waveguides

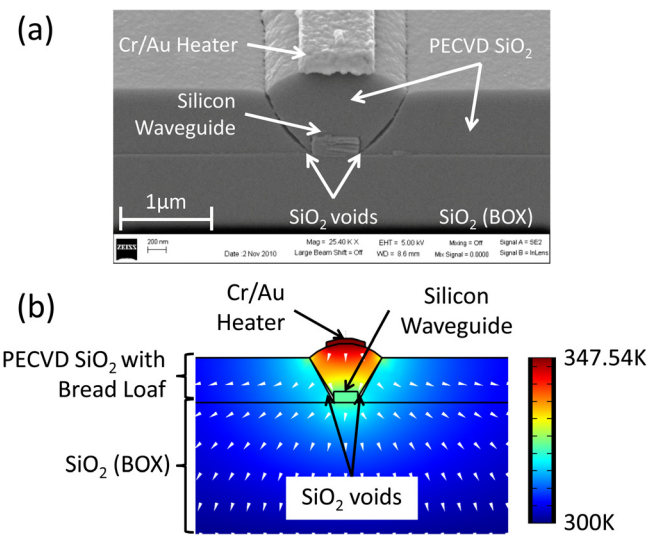

FIG. 4. (Color online) (a) SEM cross section of a heater over its waveguide. (b) COMSOL MULTIPHYSICS simulation of the thermal profile of the microheater and waveguide cross section with bread loafing of the oxide.

by reducing lateral heat transfer, and, therefore, reducing the required power for phase shifting. To accurately characterize the phase perturbations of the thermo-optical modulators, we fabricated Mach-Zehnder (MZ) modulators alongside the OPA devices with dimensions identical to the OPA with regard to waveguide and heater geometry. We experimentally confirmed a switching power of $P_\pi = 12.4$ mW along with a switching time of 9.8 μs which corresponds to a steering speed of 100 kHz.

TE polarized light at 1550 nm from a polarization maintaining lensed fiber (PMF) with a 2.5 μm output mode diameter was coupled into the input waveguide. An infrared (IR) camera connected to a variable objective lens captured the top-down far field image at the end of the silicon planar guide.

For active beam steering, we first set the input voltages to thermo-optically modulate the array phases in such a way that the electrical power applied to the micro-heaters, and, therefore, the applied phase shift of the corresponding array element, is linearly proportional to the distance of the element from the origin. Figure 5(a) demonstrates the measured beam steering angle at the edge of the silicon planar guide, along with the theoretical steering angles as a function of the electrical power to the outermost array element, which needs the largest phase shift. The required electrical input power is calculated using the phase shift data from the MZ test. As shown in Figure 5(a), when the steering angle increases, the power required for beam steering without reset becomes prohibitively large for our voltage source and limits us to a steering angle of 2.5° inside the silicon planar guide. Figure 5(a) also shows beam steering angles achieved with reset by applying modulo 2π phase shifts to the independently controlled electrodes. We were able to steer the beam at 10.2° inside the silicon planar guide equivalent to an effective angle of 31.9° in air as predicted by Snell's Law, with SLL better than −3 dB, while limiting the maximum power per channel to less than $P_{2\pi} = 24.8$ mW.

Using a similar technique as in Ref. 12, the OPA far field is observed and is used to characterize its output performance. Figures 5(b) and 5(c) demonstrate the OPA performance characterization based on the power efficiency and SLL as functions of the measured steering angle, respectively. The power efficiency is calculated by integrating the intensity over the angle interval that constitutes the main lobe (within $1/e^2$ of the maximum beam intensity). The resulting is then normalized to intensity integrated over −90° to +90°. From the simulations, we expect −4 dB SLL at 10.2°. The degradation in the performance is due to the variation in $P_{2\pi}$ of the micro-heaters, which results in increasing inaccuracies in the applied phase shift as the number of resets increases at larger steering angles. Using the effective index of the planar guide, $n_{eff} = 2.9$, we determine that the 10.2° steering in the planar guide corresponds to a steering angle in free space of 31.9°.

In summary, using a silicon nanomembrane based unequally spaced 1×12 waveguide array for actively tuned OPA that relaxes the strict waveguide spacing requirement for large angle beam steering, we have demonstrated a steering angle in free space of 31.9° at 1.55 μm wavelength. Our optical beam steering system is fabricated on SOI using CMOS compatible processes. Phase modulation is achieved thermo-optically via the use of thin-film metal heaters that are independently controlled. We have demonstrated that low-power optical beam steering is possible by applying modulo 2π phase shifts to the independently controlled electrodes. The steering speed is determined by the TO phase shifting mechanism and is 100 KHz using the TO effect, which is 2 orders of magnitude larger than LC OPAs.

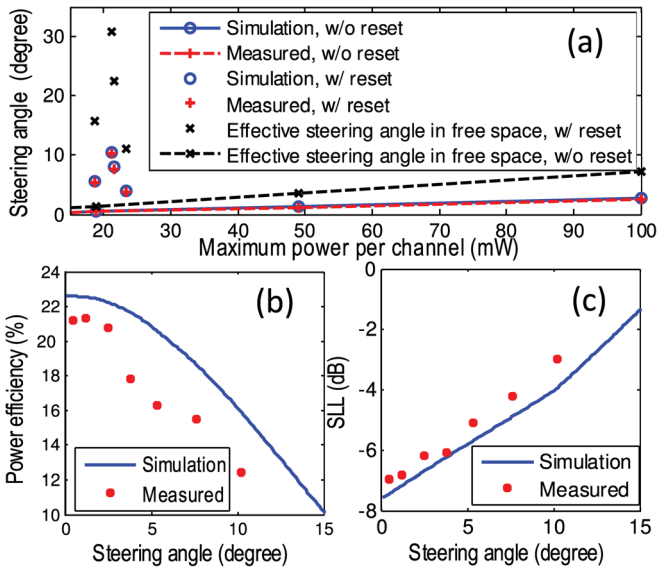

FIG. 5. (Color online) Far field characterization, (a) simulated and measured steering angle versus maximum power per channel. Effective steering angles in free space are determined from measurement data. (b) Power efficiency versus steering angle and (c) side-lobe-level versus steering angle.

This research is supported by the Multi-disciplinary University Research Initiative (MURI) program through the AFOSR, Contract No. # FA 9550-08-1-0394.

[1]Y. Pétremand, P.-A. Clerc, M. Epitaux, R. Hauffe, W. Noell, and N. F. de Rooij, Proc. SPIE **6715**, 671502 (2007).
[2]P. F. McManamon, T. A. Dorschner, D. L. Corkum, L. J. Friedman, D. S. Hobbs, M. Holz, S. Liberman, H. Q. Nguyen, D. P. Resler, R. C. Sharp, and E. A Watson, Proc. IEEE **84**(2), 268 (1996).
[3]X. Wang, B. Wang, J. Pouch, F. Miranda, J. E. Anderson, and P. J. Bos, Opt. Eng. **43**, 2769 (2004).
[4]X. Wang, B. Wang, P. Bos, P. F. McManamon, J. J. Pouch, F. A. Miranda, and J. E. Anderson, J. Appl. Phys. **98**, 073101 (2005).
[5]A. Hosseini, D. N. Kwong, Y. Zhao, Y.-S. Chen, F. Crnogorac, R. F. W. Pease, and R. T. Chen, IEEE J. Sel. Topics Quantum Electron. **15**(5), 1439 (2009).
[6]M. Jarrahi, R. F. W. Pease, D. A. B. Miller, and T. H. Lee, J. Vac. Sci. Technol. B **26**, 2124 (2008).
[7]K. V. Acoleyen, W. Bogaerts, J. Jágerská, N. Le Thomas, R. Houdré, and R. Baets, Opt. Lett. **34**, 1477 (2009).
[8]A. Hosseini, H. Subbaraman, D. N. Kwong, Y. Zhang, and R. T. Chen, Opt. Lett. **35**, 2864 (2010).
[9]D. N. Kwong, Y. Zhang, A. Hosseini, Y. Liu, and R. T. Chen, IET Electron. Lett. **46**(18), 1281 (2010).
[10]I. M. Soganci, T. Tanemura, K. A.Williams, N. Calabretta, T. de Vries, E. Smalbrugge, M. K. Smit, H. Dorren, and Y. Nakano, IEEE Photon. Technol. Lett. **22**(3), 143 (2010).
[11]A. Hosseini, D. N. Kwong, Ch.-Y. Lin, B. S. Lee, and R. T. Chen, IEEE J. Sel. Topics Quantum Electron **16**(1), 61 (2010).
[12]A. Hosseini, D. N. Kwong, Y. Zhang, A. Alu, and R. T. Chen, Appl. Opt. **50**(13), 1822 (2011).